JACS
JOURNAL OF THE AMERICAN CHEMICAL SOCIETY

ARTICLE

pubs.acs.org/JACS

Template Engineering Through Epitope Recognition: A Modular, Biomimetic Strategy for Inorganic Nanomaterial Synthesis

Alia P. Schoen,[†,‡] David T. Schoen,[†] Kelly N. L. Huggins,[†,‡] Manickam Adhimoolam Arunagirinathan,[†,‡] and Sarah C. Heilshorn*[,†,‡]

[†]Materials Science and Engineering, Stanford University, Stanford, California 94305, United States

[‡]Stanford Institute for Materials and Energy Science, SLAC National Accelerator Laboratory, Menlo Park, California 94025, United States

Supporting Information

ABSTRACT: Natural systems often utilize a single protein to perform multiple functions. Control over functional specificity is achieved through interactions with other proteins at well-defined epitope binding sites to form a variety of functional coassemblies. Inspired by the biological use of epitope recognition to perform diverse yet specific functions, we present a Template Engineering Through Epitope Recognition (TEThER) strategy that takes advantage of noncovalent, molecular recognition to achieve functional versatility from a single protein template. Engineered TEThER peptides span the biologic−inorganic interface and serve as molecular bridges between epitope binding sites on protein templates and selected inorganic materials in a localized, specific, and versatile manner. TEThER peptides are bifunctional sequences designed to noncovalently bind to the protein scaffold and to serve as nucleation sites for inorganic materials. Specifically, we functionalized identical clathrin protein cages through coassembly with designer TEThER peptides to achieve three diverse functions: the bioenabled synthesis of anatase titanium dioxide, cobalt oxide, and gold nanoparticles in aqueous solvents at room temperature and ambient pressure. Compared with previous demonstrations of site-specific inorganic biotemplating, the TEThER strategy relies solely on defined, noncovalent interactions without requiring any genetic or chemical modifications to the biomacromolecular template. Therefore, this general strategy represents a mix-and-match, biomimetic approach that can be broadly applied to other protein templates to achieve versatile and site-specific heteroassemblies of nanoscale biologic−inorganic complexes.

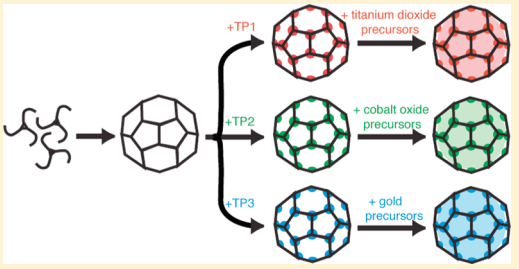

INTRODUCTION

Throughout the proteome there are numerous examples of a single parent protein performing multiple functions based on the context of the environment and the presence of binding partners, also called adaptor proteins. These adaptor proteins recognize and bind to specific sites, or epitopes, on the parent protein to create nanoscale heteroassemblies with specialized functionality. For example, mammalian cells use the protein clathrin for a variety of functions such as stabilizing the spindle apparatus during cell division,[1] packaging cargo during endocytosis,[2] and transporting biomolecules between intracellular organelles.[2] Clathrin achieves this functional versatility by interacting with a diverse family of adaptor proteins, many of which bind to a specific epitope on the clathrin molecule through a conserved amino acid sequence termed the "clathrin box".[2] A single clathrin monomer is composed of three semiflexible legs, each about 50 nm long, that form a triskelion structure with 3-fold symmetry. Individual clathrin triskelia can self-assemble into a variety of nanoscale architectures *in vitro*.[3−6]

Biotemplating, formation of inorganic materials using naturally evolved or nature-inspired materials as scaffolds for directed growth and assembly, is an attractive method to process nanomaterials due to the wide array of potential structures that may be formed.[7] Previously, clathrin cages have been used to generate nanostructures of cadmium sulfide and organoclay by relying on the intrinsic electrostatic charge of unmodified clathrin.[8] While this work demonstrated the potential of clathrin as a scaffold, using unmodified macromolecules as templates greatly limits the selection of possible template materials to those with the proper charge properties to participate in strong electrostatic interactions. Furthermore, biotemplating with unmodified macromolecules often limits the ability to localize the site of interaction, since many charged chemical groups tend to be accessible at the surfaces of biological assemblies.[9] To enable site-specific localization of interactions, macromolecular templates have been modified using several elegant genetic and chemical functionalization techniques.[10−17] However, these genetic and chemical techniques require time-consuming optimization for each desired material interaction and may result in modifications that interfere with the intrinsic self-assembly properties of the scaffold.[18]

Received: May 24, 2011
Published: October 03, 2011

dx.doi.org/10.1021/ja204732n | *J. Am. Chem. Soc.* 2011, 133, 18202–18207

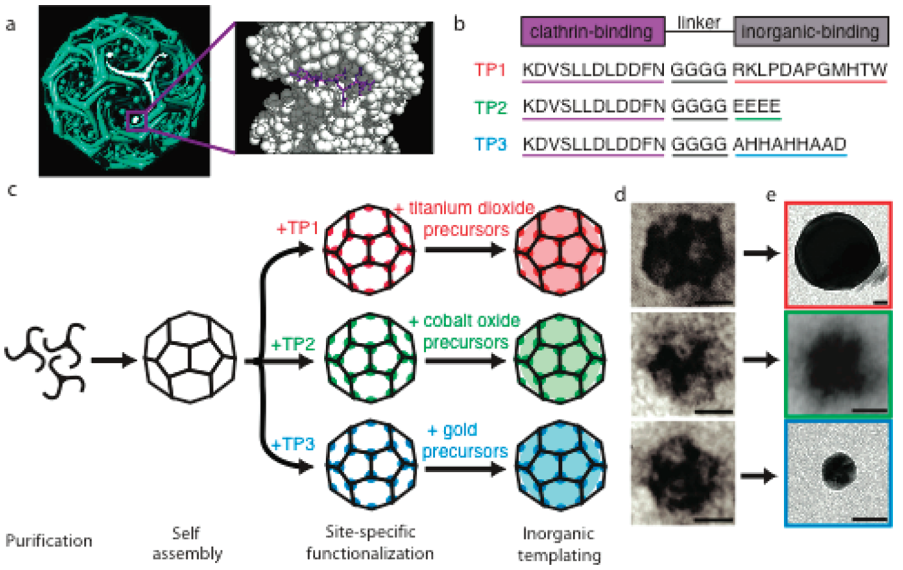

Figure 1. Versatile functionalization of clathrin cage templates using TEThER peptides. (a) Illustration of site-specific recognition of the bifunctional TEThER peptide at the clathrin monomer terminal domain. Zoomed region shows a space-fitting model of the clathrin terminal domain (white) and a stick model of the clathrin-binding peptide sequence (purple). Schematic modified from ref 2. (b) Amino acid sequences of the designed bifunctional TEThER peptides (TP). Sequence underlined in purple corresponds to the clathrin-binding peptide shown in the inset of part a. Sequences underlined in red, green, and blue represent inorganic-binding regions of TP1, TP2, and TP3, which target titanium dioxide, cobalt oxide, and gold, respectively. (c) Schematic representation of biotemplating process beginning from clathrin monomers that are assembled into cage structures and chemically fixed. Bifunctional TEThER peptides are added to locally functionalize the clathrin terminal domains inside the cage structure. Appropriate precursor molecules are added to initiate templating in solution at room temperature and pressure. (d) Representative transmission electron micrographs (TEM) of self-assembled clathrin cages stained with uranyl acetate. Scale bars = 25 nm. (e) Representative TEM micrographs of templated inorganic materials following addition of TEThER peptides and appropriate precursors to fixed clathrin cages. Titanium dioxide is outlined in red, cobalt oxide in green, and gold in blue. Scale bars = 25 nm.

To overcome these limitations, we mimic the activity of natural adaptor proteins that noncovalently assemble with a wild-type parent protein to achieve site-specific functionalization. We term this biomimetic strategy TEThER: Template Engineering Through Epitope Recognition. Our engineered "adaptor proteins" are bifunctional peptides that noncovalently bind to specific clathrin epitopes and display amino acid sequences known to interact with specific inorganic materials. By forming coassemblies of wild-type clathrin cages with these various TEThER peptides, we can extend the versatility of clathrin protein into diverse engineered functions.

Here, we design a family of TEThER peptides to customize clathrin as a scaffold for three separate inorganic templating reactions (Figure 1). Additionally, we demonstrate the three potential advantages of this noncovalent TEThER strategy compared to traditional biotemplating reactions. First, the parent protein scaffold remains unmodified; therefore, the fidelity of template self-assembly is retained. Second, epitope recognition by TEThER peptides allows site-specific functionalization at precise template binding sites. Third, since the functionalization is noncovalent, a single template can be functionalized with a variety of material-specific peptides in a mix-and-match manner, thereby enabling a variety of templating reactions. Taken together, this strategy represents a novel biomimetic approach to bridging the biologic−inorganic interface that combines localization, material specificity, and versatility in one system.

The two critical requirements for the TEThER strategy are knowledge of (1) a protein template with well-characterized binding domains available for noncovalent functionalization and (2) peptide sequences that can nucleate or interact with inorganic materials. Clathrin contains multiple epitope sites on its structure that are recognized by various adaptor proteins through specific, local peptide−protein interactions.[19,20] The "clathrin box" sequence, previously reported to be LLpL− (where L denotes leucine, p a polar amino acid, and − a negatively charged amino acid), specifically recognizes sites located at the N-terminus of the clathrin legs,[2] which are displayed on the inside of assembled 3-D cage structures (Figure 1a).[6] The structure of the clathrin box epitope along with its bound peptide ligand has been solved by X-ray crystallography[21] and reveals the presence of a pocket on the clathrin terminal domain that accommodates the long side chains of the leucine amino acids (Figure 1a, inset). Using a tetraglycine spacer for conformational flexibility, a consensus clathrin box epitope sequence was fused upstream of sequences that have been shown to interact with one of three inorganic materials, titanium dioxide,[22] cobalt oxide,[23] or gold,[24] to create TEThER peptides TP1, TP2, and TP3, respectively (Figure 1b). Because these TEThER peptides are modular in nature and many more sequences with affinity for various inorganics are available,[25−27] a mix-and-match strategy can be used to enable formation of several biologic−inorganic structures. This strategy requires no chemical or genetic modification of the underlying clathrin protein scaffold; in contrast, one simply mixes and matches assembled clathrin nanostructures with various TEThER peptides to create a variety of functional coassemblies.

RESULTS

Clathrin-coated vesicles were isolated from homogenized bovine brain tissue using differential centrifugation as previously

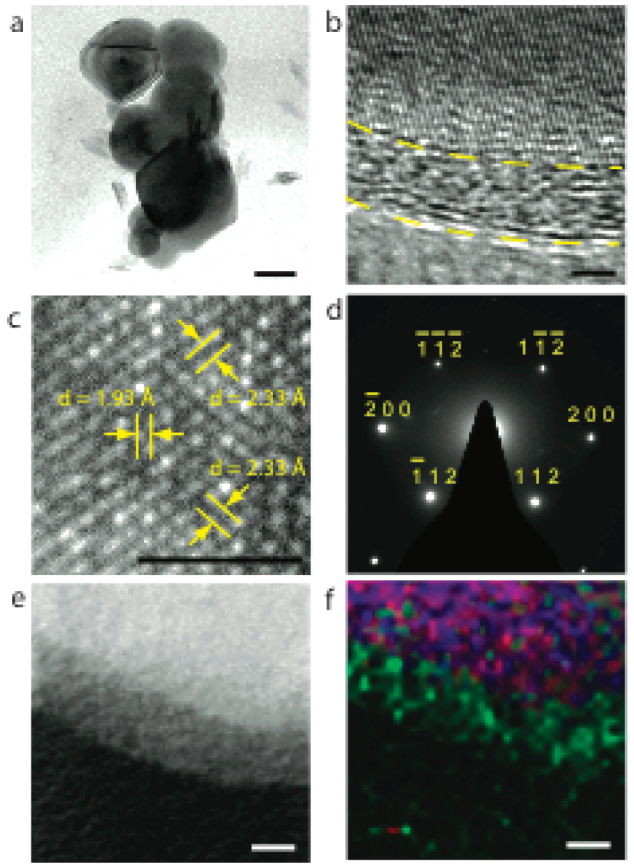

Figure 2. Cobalt oxide nanoparticles templated by TP2-functionalized clathrin cages. (a) Bright-field TEM micrograph. Scale bar = 100 nm. (b) High-resolution TEM (HRTEM) micrograph of the edge of a particle showing an amorphous carbon coating around the crystalline titanium dioxide particle. Scale bar = 2 nm. (c, d) HRTEM micrograph and electron diffraction showing measured plane spacings and assigned diffraction peaks that correspond to the anatase form of titanium dioxide. Scale bar = 2 nm. (e) Scanning TEM (STEM) dark-field micrograph of the edge of a particle. Scale bar = 2 nm. (f) Scanning energy-dispersive spectroscopy (EDS) data of the region shown in e false colored and merged to highlight the element locations (red, Ti; blue, O; green, C). Scale bar = 2 nm.

reported.[28] Size exclusion chromatography was used to separate individual clathrin triskelia from other vesicle coat proteins. Success of the protocol was analyzed by gel electrophoresis, Western blot, and mass spectrometry of the purified clathrin protein (Figure S1 in the Supporting Information). Purified clathrin triskelia were induced to self-assemble into specific structures, such as pyramidal or spherical cages (Figure S2 in the Supporting Information), by modulating the ionic strength and pH of the protein solution. Spherical clathrin cages with a mean diameter of 50 nm were formed in 100 mM 2-morpholinoethanesulfonic acid (MES), pH 6.0, and fixed with paraformaldehyde to covalently cross-link the assembled structures and prevent cage disassembly under templating reaction conditions (Figure S3 in the Supporting Information).

After fixation, one of the three engineered TEThER peptides was added to a solution of spherical clathrin cages to create functionalized coassemblies through epitope recognition. Separately, binding of TEThER peptide to the clathrin cage scaffold was verified using control peptides and a fluorescence quenching assay (Figure S4 in the Supporting Information). Upon addition of the appropriate chemical precursors, nucleation and growth of the desired inorganic material (anatase titanium dioxide, cobalt oxide, or gold) at room temperature and pressure was realized. Each of these inorganic nanomaterials is of significant interest for a variety of applications. Current technological uses of titanium dioxide nanoparticles include dye-sensitized solar cells and photocatalysis,[29] cobalt oxide has been investigated as a battery anode material,[23] and gold has been used for a variety of biomedical applications and shows interesting catalytic properties at the nanoscale.[30] Each material system yielded roughly spherical particles whose size, phase, and morphology were determined by the particular chemistry and energetics of each reaction.

To template titanium dioxide, fixed clathrin cages were combined in potassium phosphate buffer, pH 7.0, with TP1 and titanium(IV) bis(ammonium lactato) dihydroxide (TiBALDH) and analyzed by transmission electron microscopy (TEM). Crystalline nanoparticles with a mean diameter of 162 nm were observed (Figure 2a, Figure S5 in the Supporting Information). In distinct contrast, control samples replacing TP1 with cTP1 (a control peptide which does not bind to clathrin) or omitting either cages or TP1 did not contain any visible precipitate, as observed by extensive TEM (Figure S9 in the Supporting Information). These important control reactions confirm that both assembly components (i.e., clathrin cages and TP1) are required for nanoparticle synthesis. Energy-dispersive spectroscopy (EDS) confirmed the presence of titanium and oxygen in approximately a 1:2 ratio, suggesting that the particles are TiO_2. On the basis of high-resolution TEM (HRTEM) and diffraction pattern analysis, plane spacing and diffraction peaks were observed to be consistent with the unit cell of anatase TiO_2 (Figure 2c and 2d). Anatase is a photocatalytically active phase of TiO_2 and is generally not observed in this large size range. Although the anatase phase is commonly favored in solution-phase synthesis methods,[31] particles in this large size range tend to transform to the rutile phase due to differences in surface and volumetric energies between the two phases.[32] HRTEM and scanning dark-field TEM revealed an amorphous coat about 5 nm wide surrounding each particle (Figure 2b and 2e). This length scale is consistent with the predicted width of the assembled clathrin cage based on cryo-electron microscopy measurements (~5 nm).[6] EDS conducted in scanning TEM mode with a 1 nm probe size confirmed that the coat contained carbon (Figure 2f, Figure S6 in the Supporting Information). This suggests the presence of the clathrin/TP1 coassembly may serve to stabilize the anatase phase at larger particle sizes. The crystalline nature and size distribution of the particles suggests that the reaction mechanism is nucleation limited, with generally only a limited number of nuclei forming in a single assembled cage. The ensemble of nucleated particles may then undergo rapid growth until the solution is deprived of precursor, with each particle's size governed primarily by the time of the nucleation event. In support of this mechanism, we observed no evidence that the total particle size is limited by the initial diameter of the assembled protein scaffold. Despite this, the presence of the assembled protein scaffold was determined to be a required component of the reaction, as excluding the clathrin cages or the TP1 peptide did not lead to nanoparticle growth.

To demonstrate the modularity of this new templating strategy, we simply replaced TP1 with TP2 and added cobalt chloride to the fixed clathrin cages in the presence of a reducing agent (sodium borohydride) to synthesize cobalt oxide nanoparticles. The resulting nanoparticles had a mean diameter of 55 nm and exhibited a different morphology and size distribution

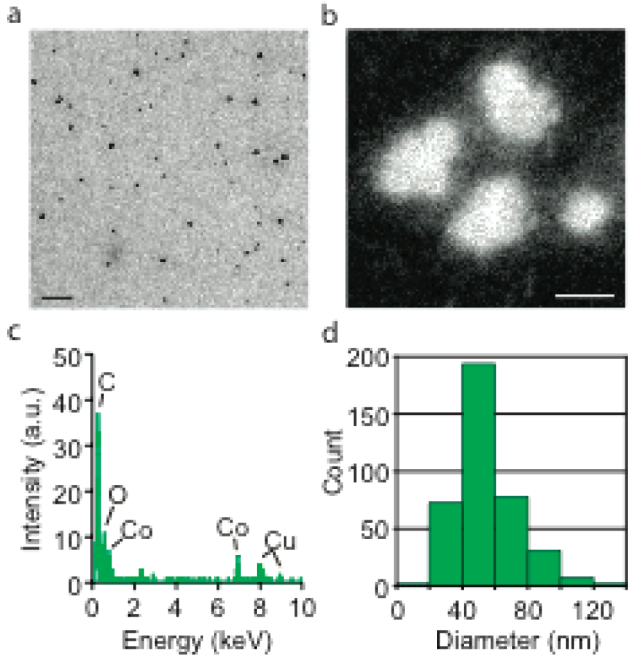

Figure 3. TP2-functionalized clathrin cages-templated cobalt oxide nanoparticles. (a) Bright-field TEM micrograph. Scale bar = 400 nm. (b) STEM dark-field micrograph. Scale bar = 100 nm. (c) EDS data confirming the presence of cobalt and oxygen. (d) Histogram (20-nm bins) showing diameter distribution of templated cobalt oxide nanoparticles.

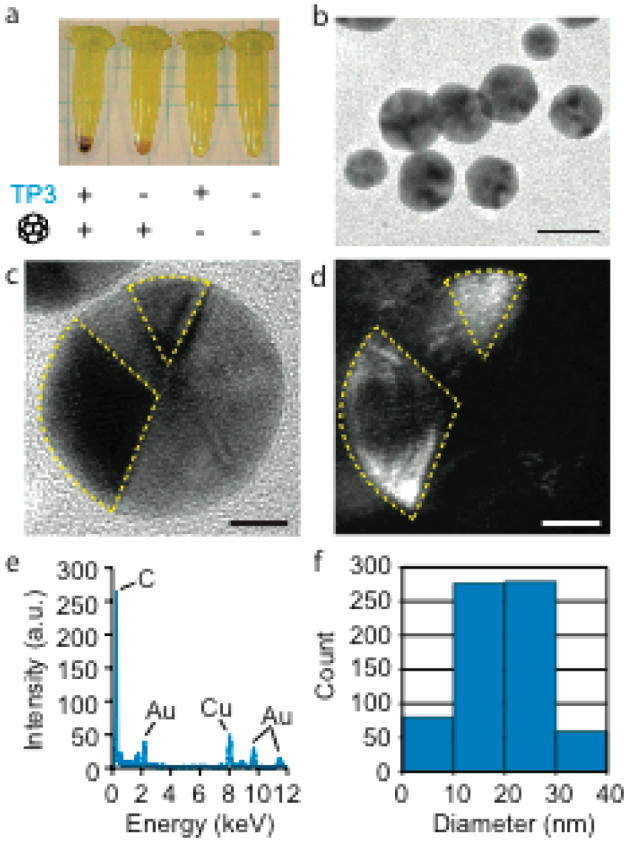

Figure 4. TP3-functionalized clathrin cages-templated gold nanoparticles. (a) Photograph of the gold templating reaction and control conditions. (b) Bright-field TEM micrograph. Scale bar = 25 nm. (c, d) Corresponding bright-field (c) and off-axis dark-field (d, using a {111} diffracted beam) TEM micrographs showing the polycrystalline nature of the gold particles. Regions outlined in yellow represent crystal grains that are well aligned with the incident beam. Scale bars = 5 nm. (e) EDS data of templated gold nanoparticles confirming the presence of gold. (f) Histogram (10-nm bins) showing the diameter distribution of templated gold nanoparticles.

compared to the anatase titanium dioxide nanoparticles (Figure 3). EDS confirmed the presence of cobalt and oxygen (Figure 3c). Similar particles were not observed in control samples replacing TP2 with cTP2 (a control peptide which does not bind to clathrin) or omitting either fixed clathrin cages or TP2 peptides. As expected, for these control reactions, all of which included a reducing agent, micrometer-sized irregular particles were observed (Figure S9 in the Supporting Information). These data demonstrate that both components of the coassembly are necessary for the nanoscale templating reaction; however, due to the need for extensive plasma cleaning of the sample prior to imaging and analysis, direct evidence of the clathrin cages was not obtained. Furthermore, replacing TP2 with TP1 in the presence of the cobalt precursor did not result in synthesis of cobalt oxide nanoparticles, indicating that TP1 is unable to interact with cobalt efficiently and the TEThER strategy can be used to specify specific inorganic reactions. It has been suggested previously that the carboxylic acid side chain of glutamic acid binds to positive cobalt ions via ion exchange, and once reduced to cobalt, these provide nucleation sites for further growth of cobalt particles that are oxidized in solution.[23,33] No crystalline domains could be detected in our particles; this observation is consistent with partial oxidation leading to an amorphous particle. In contrast to the mechanism of titanium dioxide synthesis, we believe the cobalt oxide synthesis is growth limited. Several cobalt nuclei may form inside each cage, growing until they merge into a single particle. Partial oxidation eliminates the internal grain structure; however, evidence for multiple nucleation events is preserved in the observed scalloped morphology, which has also been observed in cobalt oxide particles grown using glutamic acid residues available inside nonmodified ferritin cages.[33]

To confirm that the TEThER strategy is not limited to oxide materials, we also demonstrated the growth of noble metal nanoparticles. Fixed cages resuspended in potassium phosphate buffer, pH 7.0, were mixed with TP3 and chloroauric acid ($HAuCl_4$). Control samples without clathrin cages or without TP3 peptide were run in parallel, and all samples were incubated overnight in the dark to prevent photoreduction. Distinct color differences were observed between samples, with clear visual evidence of enhanced particle formation observed in the sample containing clathrin and TP3 (Figure 4a). TEM and EDS analysis of this sample revealed polycrystalline, round gold nanoparticles with an average diameter of 20 nm (Figure 4b–f). Cryo-TEM images clearly show the presence of gold particles within the clathrin cages (Figure S7 in the Supporting Information). Similar to the cobalt oxide synthesis described above, the imidazole side chains of histidine are presumed to capture the gold ions, which then act as nucleation sites for particle growth after reduction.[34] Because gold is inert, oxidation does not occur and the integrity of the crystalline domain is preserved. The control reactions with no cages or peptide and with peptide alone did not exhibit a color change, and no precipitate was detected by TEM. The control reaction with cages alone contained polycrystalline, irregularly shaped gold nanoparticles with an average diameter of 217 nm (Figure S8 in the Supporting Information). Therefore, unlike the previous two examples, the TEThER peptide was not necessary

to generate gold nanoparticles, though the presence of TP3 significantly altered the particle morphology and resulted in a more uniform shape and size distribution. It has been suggested that the histidine-rich peptide sequence used in TP3 acts as a surface-capping agent to stabilize gold clusters and passivate the surface.[24] Presumably, the exposed amino acids in the clathrin cage cavity are themselves interacting with gold ions even when TP3 is not present; however, the cages alone cannot inhibit continued growth in the same manner as the coassembly of cages with TP3 peptides. This hypothesis is consistent with the observation of larger particles formed in the presence of non-functionalized clathrin cages compared to the smaller particles that were observed from TP3-modified clathrin cage reactions.

DISCUSSION

By mimicking the naturally evolved strategy of modifying clathrin function through coassemblies with other proteins, we designed three new coassemblies that enabled the synthesis of three different inorganic materials (both metal and metal oxides), all in mild solutions and at ambient conditions. This versatile approach makes use of the available epitope binding sites on the clathrin terminal domain to achieve site-specific, noncovalent modification of the scaffold without requiring chemical or genetic alterations. This is a fast and flexible method to develop multiple inorganic nanostructures from a single protein scaffold using green chemistry techniques. Several additional epitope binding sites are present on other regions of the clathrin protein and may enable simultaneous specific interactions with multiple inorganic materials at distinct locations (e.g., on the outer cage surface in addition to within the inner cavity). The structural variety of self-assembled clathrin, which includes spherical and pyramidal cages as well as hexagonal and cubic lattices,[3,4] makes it an attractive target for further developing biotemplating protocols. For example, noncovalent modification of protein lattices can be used to direct the arrangement of colloidal nanoparticles into extended arrays.[35]

Because the TEThER strategy does not require chemical or genetic modification of the wild-type protein scaffold, this method can be easily extended to other protein coassemblies. Nature presents us with a vast range of naturally occurring complex structures that could be directly used as starting materials for noncovalent TEThER functionalization. Furthermore, the TEThER strategy enables the use of a single wild-type protein scaffold to template multiple inorganic syntheses in a mix-and-match manner. Therefore, the ever-expanding library of inorganic synthesis peptides will enable formation of a wide variety of materials. In summary, TEThER is a powerful biomimetic strategy that can be broadly applied to generate a multitude of diverse organic−inorganic nanostructures.

MATERIALS AND METHODS

Clathrin cages were assembled by dialyzing clathrin monomers into 4 mM Tris buffer at pH 7.0 adding 1/10 volume of 1 M MES, pH 6.0. The protocol for clathrin purification is available in the Supporting Information. Samples were spun down at 16 000*g* for 10 min, decanted, then resuspended with 100 mM MES, pH 6.0. Paraformaldehyde (16%) was added to a final concentration of 4%, and the samples were fixed at room temperature. After spinning at 16 000*g* for 10 min and decanting, 100 mM potassium phosphate, pH 7.0, was added to dissociate unfixed cages. Samples were spun at 16 000*g* for 10 min a final time and decanted to obtain fixed clathrin cages.

Fixed clathrin cages resuspended in 100 mM potassium phosphate, pH 7.0, were incubated with TP1 peptide (1 mg/mL final concentration, GenScript) for 15 min. Samples omitting either clathrin cages or TP1 were run in parallel. TiBALDH was added to 2.5 wt %, and the solution was allowed to react for 2 h and then centrifuged at 16 000*g* for 10 min. The resulting pellet was rinsed 4 times with water and then resuspended in water.

Fixed clathrin cages resuspended in 2 mM cobalt chloride, pH 6.0, were incubated with either TP1, TP2, or no peptide (1 mg/mL final concentration, GenScript) for 1 h. Samples omitting clathrin cages were run in parallel. Sodium borohydride (7.5 mM final concentration) was added, and the solution was allowed to react for 10 min and then centrifuged at 16 000*g* for 10 min. The resulting pellet was rinsed 4 times with water and then resuspended in water.

Fixed clathrin cages resuspended in 100 mM potassium phosphate, pH 7.0, were incubated with TP3 peptide (1 mg/mL final concentration, GenScript) for 15 min. Samples omitting clathrin cages or TP3 were run in parallel. $HAuCl_4$ was added to 4 mM, and the solutions were allowed to react in the dark overnight.

Samples were drop cast onto carbon type-B, 400 mesh, copper TEM grids (Ted Pella) after extensive washing of the precipitated material with the exception of the gold samples which were directly drop cast from their reaction solutions. TEM was performed either on a JEOL JEM-1230 operated at 80 kV or an FEI Tecnai G2 F20 X-TWIN operated at 200 kV. EDS was carried out in the Tecnai using an EDAX Analyzer for elemental analysis. Image analysis was performed using ImageJ.

ASSOCIATED CONTENT

Supporting Information. Details of protein purification, cross-linked clathrin cage characterization, control peptides, and related experiments and Figures S1−S9. This material is available free of charge via the Internet at http://pubs.acs.org.

AUTHOR INFORMATION

Corresponding Author
heilshorn@stanford.edu

ACKNOWLEDGMENT

We thank Andrew Spakowitz, Nick Melosh, Seb Doniach, and the staff at the Cell Sciences Imaging Facility and Stanford Nanocharacterization Laboratory for helpful discussions. We thank Yifan Cheng, University of California, San Francisco, for use of cryo-TEM facilities. A.P.S. acknowledges support from a Stanford Bio-X fellowship. D.T.S. acknowledges support from NDSEG and NSF GRFP fellowship programs. This work is supported by the American Chemical Society Petroleum Research Fund, 49534-DNI10 (nanoparticle self-assembly), and the Department of Energy, Office of Basic Energy Sciences, Division of Materials Sciences and Engineering, under contract DE-AC02-76SF00515 (inorganic synthesis).

REFERENCES

(1) Royle, S.; Bright, N.; Lagnado, L. *Nature* **2005**, *434*, 1152–1157.
(2) Kirchhausen, T. *Annu. Rev. Biochem.* **2000**, *69*, 699–727.
(3) Heuser, J.; Keen, J.; Amende, L.; Lippoldt, R.; Prasad, K. *J. Cell Biol.* **1987**, *105*, 1999–2009.
(4) Sorger, P.; Crowther, R.; Finch, J.; Pearse, B. *J. Cell Biol.* **1986**, *103*, 1213–1219.
(5) Zhang, F.; Yim, Y.-I.; Scarselletta, S.; Norton, M; Eisenberg, E.; Greene, L. E. *J. Biol. Chem.* **2007**, *282*, 13282–13289.

(6) Fotin, A.; Cheng, Y.; Sliz, P.; Grigorieff, N.; Harrison, S. C.; Kirchhausen, T.; Walz, T. *Nature* **2004**, *432*, 573–579.
(7) Dickerson, M. A.; Sandhage, K. H.; Naik, R. R. *Chem. Rev.* **2008**, *108*, 4935–4978.
(8) Sadasivan, S.; Patil, A. J.; Bromley, K. M.; Hastie, P. G. R.; Banting, G.; Mann, S. *Soft Matter* **2008**, *4*, 2054–2058.
(9) Pace, C. N.; Grimsley, G. R.; Scholtz, J. M. *J. Biol. Chem.* **2009**, *284*, 13285–13289.
(10) Bai, H.; Xu, F.; Anjia, L.; Matsui, H. *Soft Matter* **2009**, *5*, 966–969.
(11) Lee, Y. J.; Yi, H.; Kim, W.-J.; Kang, K.; Yun, D. S.; Strano, M. S.; Ceder, G.; Belcher, A. M. *Science* **2009**, *324*, 1051–1055.
(12) Sano, K.; Sasaki, H.; Shiba, K. *J. Am. Chem. Soc.* **2006**, *128*, 1717–1722.
(13) Behrens, S.; Heyman, A.; Maul, R.; Essig, S.; Steigerwald, S.; Quintilla, A.; Wenzel, W.; Bürck, J.; Dgany, O.; Shoseyov, O. *Adv. Mater.* **2009**, *21*, 3515–3519.
(14) Wang, Q.; Kaltgrad, E.; Lin, T.; Johnson, J.; Finn, M. *Chem. Biol.* **2002**, *9*, 805–811.
(15) Hooker, J.; Kovacs, E.; Francis, M. *J. Am. Chem. Soc.* **2004**, *126*, 3718–3719.
(16) Uchida, M.; Klem, M. T.; Allen, M.; Suci, P.; Flenniken, M.; Gillitzer, E.; Varpness, Z.; Liepold, L. O.; Young, M.; Douglas, T. *Adv. Mater.* **2007**, *19*, 1025–1042.
(17) Anderson, E. A.; Isaacman, S.; Peabody, D. A.; Yang, E. Y.; Canary, J. W.; Kirshenbaum, K. *Nano Lett.* **2006**, *6*, 1160–1164.
(18) Bruckman, M. A.; Soto, C. M.; McDowell, H.; Liu, J. L.; Ratna, B. R.; Korpany, K. V.; Zahr, O. K.; Szuchmacher Blum, A. *ACS Nano* **2011**, *5*, 1606–1616.
(19) Dell'Angelica, E.; Klumperman, J.; Stoorvogel, W.; Bonifacino, J. *Science* **1998**, *280*, 431–434.
(20) Knuehl, C.; Chen, C.-Y.; Manalo, V.; Hwang, P. K.; Ota, N.; Brodsky, F. M. *Traffic* **2006**, *7*, 1688–1700.
(21) ter Haar, E.; Harrison, S.; Kirchhausen, T. *Proc. Natl. Acad. Sci. U.S.A.* **2000**, *97*, 1096–1100.
(22) Sano, K.-I.; Yoshii, S.; Yamashita, I.; Shiba, K. *Nano Lett.* **2007**, *7*, 3200–3202.
(23) Nam, K. T.; Kim, D.-W.; Yoo, P. J.; Chiang, C.-Y.; Meethong, N.; Hammond, P. T.; Chiang, Y.-M.; Belcher, A. M. *Science* **2006**, *312*, 885–888.
(24) Slocik, J.; Moore, J.; Wright, D. *Nano Lett.* **2002**, *2*, 169–173.
(25) Sarikaya, M.; Tamerler, C.; Jen, A.; Schulten, K.; Baneyx, F. *Nat. Mater.* **2003**, *2*, 577–585.
(26) Kacar, T.; Ray, J.; Gungormus, M.; Oren, E. E.; Tamerler, C.; Sarikaya, M. *Adv. Mater.* **2009**, *21*, 295–299.
(27) Shiba, K. *Curr. Opin. Biotechnol.* **2010**, *21*, 412–425.
(28) Jackson, A. P. In *Methods in Molecular Biology, Biomembrane Protocols: I Isolation and Analysis*; Graham, J. M., Higgins, J. A., Eds.; Humana Press, Inc.: Totowa, NJ, 1993; Vol. 19, pp 83−96.
(29) Diebold, U. *Surf. Sci. Rep.* **2003**, *48*, 53–229.
(30) Daniel, M.-C.; Astruc, D. *Chem. Rev.* **2004**, *104*, 293–346.
(31) Reyes-Coronado, D.; Rodriguez-Gattorno, G.; Espinosa-Pesqueira, M. E.; Cab, C.; de Coss, R.; Oskam, G. *Nanotechnology* **2008**, *19*, 145605–145614.
(32) Zhang, H.; Banfield, J. *J. Mater. Chem.* **1998**, *8*, 2073–2076.
(33) Kim, J.-W.; Choi, S. H.; Lillehei, P. T.; Chu, S.-H.; King, G. C.; Watt, G. D. *Chem. Commun.* **2005**, 4101–4103.
(34) Djalali, R.; Chen, Y.; Matsui, H. *J. Am. Chem. Soc.* **2003**, *125*, 5873–5879.
(35) Shindel, M. M.; Mohraz, A.; Mumm, D. R.; Wang, S.-W. *Langmuir* **2009**, *25*, 1038–1046.